JOURNAL OF THERMOPHYSICS AND HEAT TRANSFER
Vol. 15, No. 3, July–September 2001

Temperature Dependence of Thermophysical Properties of Disodium Hydrogenphosphate Dodecahydrate

Satoshi Hirano*
National Institute of Advanced Industrial Science and Technology, Tsukuba 305-8569, Japan
Takeo S. Saitoh†
Tohoku University, Sendai 980-8579, Japan
and
Masaaki Oya* and Masakazu Yamazaki*
National Institute of Advanced Industrial Science and Technology, Tsukuba 305-8569, Japan

The temperature dependence of thermophysical properties was evaluated for disodium hydrogenphosphate dodecahydrate, which is used in long-term, supercooled thermal energy storage (Super-TES). Super-TES stores thermal energy at temperatures lower than the melting point of the phase-change material, which reduces heat loss from the storage system. Although the degree of supercooling depends not only on the intensive material properties, such as phase-change temperatures, but also on extensive properties, such as the total material volume, except for distilled water and metals there is insufficient information in the open literature on supercooling phenomena to develop heat storage devices. A promising material for Super-TES applications is disodium hydrogenphosphate dodecahydrate. The thermophysical properties of disodium hydrogenphosphate dodecahydrate are evaluated, and its suitability for Super-TES applications is clarified. We found that in the liquid phase the hydrate density and viscosity decrease monotonically with increasing temperature. We also found that the specific heat in the liquid phase (3.45 kJ/kg · K) and the thermal conductivity in the solid phase (1.01 W/m · K near the melting point) were twice as large as reported in the open literature. This indicates that this hydrate is useful for storing both latent and sensible heat, for reducing heat loss from energy storage systems, and for efficiently exchanging energy between heat sources and the hydrate.

Nomenclature

c_p = specific heat at constant pressure, kJ/kg · K
T = temperature, °C
η = viscosity, Pa · s
λ = thermal conductivity, W/m · K
ρ = density, kg/m^3

Subscripts

l = liquid phase
s = solid phase

Introduction

GLOBAL warming and depletion of fossil fuels are two problems that are caused by large-scale energy consumption. To resolve these problems, the current practice of focusing on inexpensive energy use should be abandoned, and the focus should be shifted to efficient energy use that does not adversely affect nature. Thermal energy storage is important for the efficient generation and use of energy because it can store energy during slack demand times, for example, at night, and provide energy during high demand times, for example, during the day. To meet a given peak demand, energy storage permits smaller power plants to be built, and it also permits them to be run continually at peak operating efficiency. Such energy storage devices are also important for smoothing out power-generation cycles for solar and wind power generation, where power can only be produced during daylight (solar power) or under windy (wind power) conditions.

Two types of thermal energy storage are now in use: sensible heat thermal energy storage (SHTES) and latent heat thermal energy storage (LHTES). LHTES uses a phase-change material (PCM) and is desirable because, compared with SHTES, LHTES systems transfer energy at constant temperature during a phase change, permitting high-energy storage density and stable output temperature. Therefore, for applications where the space used by such systems must be minimized, LHTES is more suitable than SHTES. Whereas most LHTES systems are developed for short-term storage, in this work we considered the possibility of using the supercooling behavior of PCMs to develop long-term LHTES systems.

Figure 1 shows typical temporal temperature variations for the solidification of one type of PCM, disodium hydrogenphosphate dodecahydrate ($Na_2HPO_4 \cdot 12H_2O$). From the liquid phase, this hydrate is cooled at a constant rate of 0.3°C/min in a test tube submersed in a water bath. Although the melting point of the hydrate is about 36°C, crystallization does not start until the liquid is supercooled to 23°C. Once crystallization starts, the temperature of the hydrate rises to its melting point, and the hydrate releases energy, equal to its heat of fusion, until solidification is completed.

Supercooled thermal energy storage (Super-TES) uses this temperature hysteresis between fusion and solidification to store energy. A typical operating mode of Super-TES is as follows. The PCM is completely melted by using surplus heat in the summer and is left at room temperature without thermal insulation until winter. In the winter, the supercooled PCM is crystallized on demand, and the heat of fusion released from the PCM at a temperature higher than room temperature is used as an energy source. Therefore, compared with conventional storage systems, Super-TES systems can reduce heat loss from the storage system because energy is stored at a temperature close to room temperature.

Because the degree of supercooling strongly depends on both the intensive and extensive material properties,[1] the material properties must be known to design properly thermal energy storage systems.

Presented as Paper 2000-2979 at the 35th Intersociety Energy Conversion Engineering Conference, Las Vegas, NV, 23–27 July 2000; received 23 August 2000; revision received 2 March 2001; accepted for publication 21 March 2001.

*Senior Researcher, Institute for Energy Utilization. 16-1 Onogawa.
†Professor, Department of Aeronautics and Space Engineering. 01, Aramaki-Aoba.

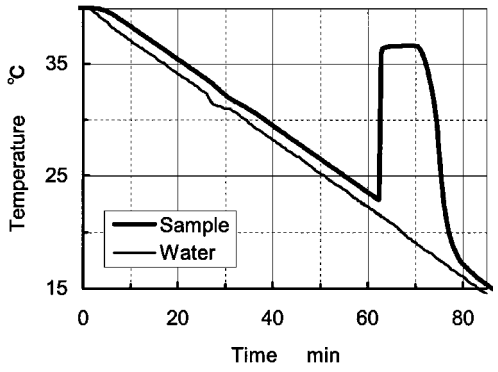

Fig. 1 Temporal temperature variation of $Na_2HPO_4 \cdot 12H_2O$ during constant-rate cooling; increase near 60 s corresponds to supercooled liquid freezing.

However, except for distilled water and metals, there is insufficient information on the thermophysical properties of hydrates. Therefore, in this work we studied the thermophysical properties of disodium hydrogenphosphatedodecahydrate.

Materials and Methods

Overview

Disodium hydrogenphosphatedodecahydrate is a promising material for Super-TES because it is less toxic and cheaper than most other hydrates. The probability that nucleus formation is initiated in the supercooled hydrate by physical vibration and the possibility that disodium hydrogenphosphate segregates from the hydrate are also lower than for most other hydrates. The melting point of the hydrate also makes it suitable for space heating.

To optimize the operating temperature and size of thermal energy storage systems, the melting point and heat of fusion are the two most important thermophysical properties of PCMs. The solid and liquid densities are also useful for estimating thermal expansion of PCMs and nuclei formation conditions. The specific heat also required to optimize the size of storage systems. Large specific heat permits the use of sensible heat of PCMs in addition to latent heat. Thermal conductivity is useful for evaluating heat transfer rate among PCMs, surroundings, and working fluids for storing and restoring thermal energy. Viscosity is useful for evaluating convection intensity and growth rate of crystals in PCMs. Therefore, in this work we measured these thermophysical properties of the hydrate within the temperature range most likely to be used for Super-TES systems.

Materials

We used special reagent-grade disodium hydrogenphosphate dodecahydrate conforming to Japanese Industrial Standard (JIS) K9019-1996. The chemical content is listed in Table 1. Except for the specific heat measurements, all measurements were made with the hydrate of the same product lot. Only for the measurement of the specific heat, hydrate made by another manufacturer was also used to verify the measurement. The additional hydrate also conforms to JIS K9019-1996.

Disodium hydrogenphosphate dodecahydrate is efflorescent, which means that in air the water of the hydrate evaporates and dodecahydrate changes into heptahydrate or dihydrate. The hydrate must, therefore, be isolated from room air. Except for measurement of the hydrate viscosity, all measurements were done in a sealed vessel of fixed capacity. One side effect of this is that pressure changes caused by phase changes and thermal expansion were included in the measured specific heat. Therefore, we also determined the effect of containment of the hydrate on the evaluation of the specific heat.

Melting Point and Heat of Fusion

The melting point and heat of fusion of seven samples were measured with a power compensation differential scanning calorimeter (DSC). The DSC was calibrated with indium before the measurement. Each sample weighed 7 mg. These samples were encapsulated by using aluminum sample pans. The capsules had an effective volume of 20 μl and could withstand an internal pressure of 0.2 MPa (gauge). The heating rate of the sample was 5.0°C/min, which is a typical scanning rate for DSCs.

To test if reactions occurred between the hydrate and the container, we compared measurements made with and without a polytetrafluoroethylene liner, which prevents the hydrate from reacting with the container.

Table 1 Chemical composition of $Na_2HPO_4 \cdot 12H_2O$ (JIS K9019-1996)

Purity	Minimum 99.0%
pH (50 g/l, 25°C)	9.0 – 9.4
Chloride	Maximum 0.001%
Sulfate	Maximum 0.005%
Heavy metals (as Pb)	Maximum 0.001%
Calcium	Maximum 0.02%
Arsenic	Maximum 1 ppm
Iron	Maximum 5 ppm
Ammonium	Maximum 0.001%

Density

We measured the sample density with a 20-ml graduated cylinder and an electronic balance. We used an average density calculated from four measurements. Before the measurements, we calibrated the graduated cylinder by filling it with distilled water of known density (the temperature dependence of the density and the uncertainty are given in Refs. 2 and 3), weighing it, and back calculating the equivalent volume. The cylinders were immersed in a water bath, and the water temperature was measured with a platinum resistance thermometer accurate to within ±0.11°C.

We measured the solid-phase density by using samples that were crystallized very slowly from the bottom up, which results in compact crystals. Because crystallization progressed near the melting point, the measured values were considered to be the solid density at the melting point.

Specific Heat

To measure c_p, we calibrated the DSC with synthetic sapphire, whose c_p is given in Ref. 4, and then used the calibrated DSC to measure c_p of the hydrate. The weight of the hydrate sample used for the measurement was the same as the weight of the reference sapphire used for calibration. The samples were encapsulated by using O-ring-sealed stainless-steel sample pans. The capsules had an effective volume of 60 μl and could withstand an internal pressure of 2.4 MPa (gauge).

To check the accuracy of our method for measuring c_p, we measured c_{pl} of distilled water and compared it with the reference value given in Ref. 5.

Thermal Conductivity

The thermal conductivity of the sample was measured by using the transient plane source (TPS) technique. Using the TPS technique with a single sensor, the thermal conductivity of both the solid and liquid phases can be measured. The sensor was made of nickel foil with a diameter of 6.6 mm and a thickness of 10 μm. Both sides of the sensor were coated with a 30-μm-thick polyimide film.

When the thermal conductivity of the sample in the solid phase was measured, the sensor was sandwiched between two blocks of the sample, and the blocks were bound with rubber bands to compensate for thermal shrinkage of the sample. When the thermal conductivity of the sample in the liquid phase was measured, the sensor was immersed vertically into the sample.[6] The measurement was made in an environmentally controlled chamber. With the TPS technique, the change of electrical resistance of the nickel sensor was measured while a constant electric current was supplied to the sensor for a defined period of time. The thermal conductivity was calculated from

the input power to the sensor and the temperature rise of the sensor. The details of the TPS technique are described elsewhere.[7–9] The temperature of the sample was measured with a copper–constantan thermocouple accurate to ±0.2°C.

We used heating periods of 2.5 s for the liquid phase and 20 s for the solid phase. The temperature rise of the sensor was about 1.0°C during this period. This short heating period suppresses the measurement error caused by natural convection in liquid samples. The small temperature rise suppresses the measurement error caused by heterogeneous heat transfer along edges of the solid samples. To calibrate our TPS system, we measured the thermal conductivities of distilled water and clear quartz and compared the measured values with reference values.

Viscosity

The viscosity of the sample in the liquid phase was measured with a rotational viscometer. The cylindrical spindle of the viscometer was 25.2 mm in diameter, the effective length was 92.4 mm, and the sample size was 16 ml. The wire that suspends the spindle from the electric motor was 1 mm in diameter. The rotational speed for measuring the viscosity was varied from 10 to 60 rpm. The resulting shear rate ranged from 12.23 to 73.38 1/s. The temperature of the sample was measured with a thermistor resistance thermometer accurate to ±0.07°C.

To prevent evaporation of the sample, 1.5 ml of silicone oil was carefully placed on the surface of the sample by using a syringe. Because the density of silicone is about 930 kg/m^3 at 25°C and the hydrate is insoluble in silicone, the silicone formed a thin layer on the sample. The resulting thickness of the silicone layer was 2.5 mm. We also measured the viscosities of water with and without the silicone layer to clarify the influence of the silicone on the viscosity measurements.

Results and Discussion

Melting Point and Heat of Fusion

The measured mean melting point was 35.54°C. The probable error of the measurement was ±0.38°C, which is the sum of the calibration error of the platinum resistance thermometer of DSC of ±0.1°C and the precision error of each measurement of ±0.28°C. The quoted error in this paper is this maximum error limit. The measured heat of fusion was 265.6 kJ/kg, and the measurement error was ±3.7 kJ/kg. The purity of the hydrate used in this measurement was estimated to be 99.66% (+0.28/−0.43%) by fitting a portion of the DSC data to the Van't Hoff relationship. Because no significant difference was observed between the melting points or heat of fusions measured with and without the polytetrafluoroethylene liner in the sample pan, we concluded that reactions between the hydrate and the aluminum sample pan were negligible during our measurements.

Table 2 shows a comparison of our results with reference values.[10–13] There is no information on the measurement methods used in Refs. 10 and 11. The specific heat of the hydrate in Ref. 12 originated from Ref. 13, which gives the heat of solidification of the hydrate instead of the heat of fusion. This heat of solidification was calculated from the heat released from the material during a temperature change that included solidification. The heat of solidification is sometimes less than the heat of fusion.[12] Because this method uses the specific heats in the liquid and the solid phase to calculate the heat of solidification, the value given in Ref. 13 depends on the values of the two specific heats. However, it is difficult to measure directly specific heats near the melting point because the measurement of specific heat requires a temperature change. However, for materials with impurities, the temperature change causes a phase change. Therefore, the specific heats used in Ref. 13 for evaluating the heat of solidification were not measured at temperatures close to the melting point, but were measured over a relatively wide temperature range of −21–2°C for c_{p_s} and 40–80°C for c_{p_l}. The average specific heats given in Ref. 13 are $c_{p_s} = 1.71$ kJ/kg · K and $c_{p_l} = 3.13$ kJ/kg · K. This c_{p_l} is 9.3% smaller than our measured value. The resulting effect is that when the calculated specific heat in the liquid phase is smaller than its true value, the calculated heat of solidification is larger than its true value. Table 2 shows that the melting point and the heat of fusion of this sample agree with the values from Ref. 10.

Table 2 Measured melting points and heats of fusion

Reference	Melting point, °C	Heat of fusion, kJ/kg
	$Na_2HPO_4 \cdot 12H_2O$	
This work	35.54	265.6
10	36	264
11	35	281
12, 13	36.1	280[a]
	H_2O	
This work	0.04	331.6
12	0	333.6

[a]Heat of solidification.

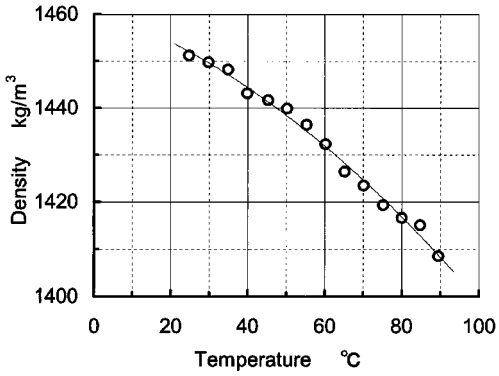

Fig. 2 Temperature dependence of liquid density of $Na_2HPO_4 \cdot 12H_2O$.

The heat of fusion of water given in Table 2 was measured with the same instrument used for the measurement of the hydrate. The measured heat of fusion of water agrees with that given in Ref. 12 and given in all other references we searched.[14–18]

Density

Figure 2 shows the average liquid density of the sample we measured as a function of temperature. The solid curve in Fig. 2 represents the least-squares approximation, expressed as

$$\rho_l = -3.289 \times 10^{-3} T^2 - 2.93 \times 10^{-1} T + 1461 \qquad (1)$$

for $25 \leq T \leq 90$°C. Measured values below the melting point, 36°C, are the densities of the supercooled state.

Because the temporal temperature fluctuation of the bath was less than ±0.05°C, the temperature fluctuation in the cylinders was also less than ±0.05°C. The resulting measurement error of the density was ±6 kg/m^3 including the calibration error. Figure 2 shows that with increasing temperature, the liquid density decreases monotonically from the supercooled to normal liquid conditions. References 10 and 11 report a hydrate liquid density of 1.45×10^3 kg/m^3 and 1.44×10^3 kg/m^3, respectively. Although there is no information on measurement methods and conditions used in Refs. 10 and 11, their reported liquid densities are equivalent to our densities measured near the melting point (Fig. 2).

The solid density that we measured was 1.52×10^3 kg/m^3, which also agree with the values from Refs. 10 and 11. This indicates that the solid density listed in Refs. 10 and 11 is the density near the melting point of 36°C.

Specific Heat

Figure 3 shows our measured values of c_p. The measured specific heat of the liquid hydrate was about the same as c_p of water and increased 3.2% for a temperature increase from 15 to 100°C. We found that $c_{p_s} \approx 0.6 c_{p_l}$ near the melting point, and that c_{p_s} was

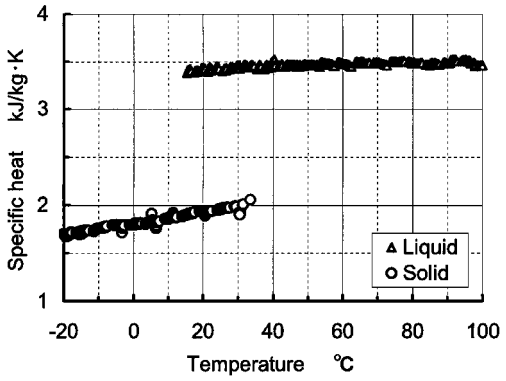

Fig. 3 Temperature dependence of specific heat of $Na_2HPO_4 \cdot 12H_2O$.

more temperature sensitive than c_{pl}. This property enhances the availability of the hydrate for PCMs because both the sensible and latent heat can be effectively used for thermal energy storage. From a polynomial fit to our data, we can express c_{ps} and c_{pl} as

$$c_{ps} = 1.739 \times 10^{-5}T^2 + 5.736 \times 10^{-3}T + 1.803 \qquad (2)$$

for $-20 \le T \le 34$°C and

$$c_{pl} = 3.23 \times 10^{-7}T^3 - 6.68 \times 10^{-5}T^2 + 5.17 \times 10^{-3}T + 3.34 \qquad (3)$$

for $15 \le T \le 100$°C.

For $T \le 60$°C, the difference between our measured values for distilled water and that given in Ref. 5 was within 1%, and for $T > 60$°C the difference was within 2%. The uncertainty in c_p of the reference sapphire was ±0.1% (Ref. 4) and the uncertainty in c_p of water was ±0.2% (Ref. 3). In the solid phase, the probable measurement error of c_p was ±1.1%, and in the liquid phase, the probable measurement error of c_p was ±1.3% for $T \le 60$°C and ±2.3% for $T > 60$°C.

The effect of the pressure change in the sample pan caused by the phase change and by thermal expansion of the material was considered in the calculation of c_p. The sample was in the solid state when it was encapsulated at $T = 25$°C and atmospheric pressure of 0.101 MPa. At the same temperature, when the sample was in the liquid state, the internal pressure inside the capsule rose to 2% above atmospheric pressure because the solid density was higher than the liquid density. When water is encapsulated in the same sample pan, the pressure increase of 2% causes a specific heat decrease of 2×10^{-4}% (Ref. 19), which is lower than the probable error of ±1.3% for this measurement. Because the boiling temperature of the hydrate was greater than or equal to that of water, the influence of the pressure change in the sample pan was negligible.

Table 3 shows a comparison of our results with reference values (Refs. 10, 11, 13, and 20–26). In Refs. 10 and 11, no information on the method for measuring the specific heat is given. Compared with Refs. 10 and 11, our measured c_{ps} were 6% higher at $T = 0$°C and 28% higher at the melting point of the hydrate, and c_{pl} was 82% larger at the melting point. The values listed in Ref. 13 were measured with a copper calorimeter. The data in Ref. 20 originated from Ref. 21, which was a provisional report of Ref. 13. Compared with the values given in Ref. 13, the average value of our measured c_{pl} for $40 \le T \le 80$°C was 9.3% higher. The data in Ref. 22 originated from Refs. 23 and 24. The values listed in the Refs. 23 and 24 were measured with a copper calorimeter in a vacuum tube. The reason for the differences in our specific heats with the reference values is unclear. One reason may be that the data given in Reference 22 are overextrapolated data from Refs. 23 and 24, because Refs. 23 and 24 report only the values listed in Table 3, and all of the data in Refs. 22–24 can be fitted with a single straight line. To determine liquid-state specific heats, Refs. 10 and 11 seem to use solid-state specific heats extrapolated past the melting point to 50°C, that is, liquid state.

Table 3 Comparison of specific heats measured in this work with values available in the open literature

Reference	Temperature, °C	Specific heat, kJ/kg · K Solid	Liquid
	$Na_2HPO_4 \cdot 12H_2O$		
This work	35.54	2.03[a]	3.45
10	——	1.6	1.9
11	——	1.7	1.9
13	−21–2	1.71[b]	——
	40–80	——	3.13[b]
20, 21	−20–2	1.90[b]	——
	44–79	——	3.17[b]
22	0	1.69	——
	50	1.94	——
23	−190	0.61	——
	−75	1.25	——
24	−75–0	1.48[b]	——
	33.5	1.56[c]	——
	H_2O		
25	−5	2.06	4.25
	$CH_3COONa \cdot 3H_2O$		
26	58	2.10[a]	3.46

[a]Extrapolated. [b]Average for the listed temperature range. [c]For undecahydrate.

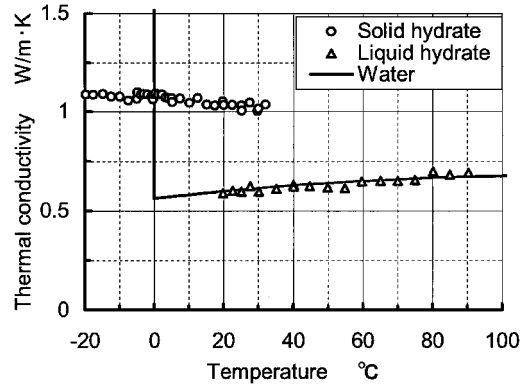

Fig. 4 Temperature dependence of thermal conductivity of $Na_2HPO_4 \cdot 12H_2O$.

Because 60 wt % of the hydrate is water, the thermophysical properties of water affect the thermophysical properties of the hydrate. As shown in Table 3, for water $c_{ps} \approx 0.5c_{pl}$ near its melting point. The specific heat for sodium acetate trihydrate near its melting point, 58°C, listed in Ref. 26 is $c_{ps} \approx 0.6c_{pl}$, similar to our measured values for the hydrate of phosphate.

The measured specific heat for disodium hydrogenphosphatedodecahydrate made by a different manufacturer was nearly the same as shown in Fig. 3. The differences of the specific heats of the two different samples were within 1.5% over the temperature range of $-20 \le T \le 100$°C. This close agreement between these two different sample hydrates indicates that the difference between the properties measured in this work and values reported elsewhere was not caused by differences in the samples.

Thermal Conductivity

Figure 4 shows our measured thermal conductivities of the hydrate. For comparison, the solid line shows the reference values of the thermal conductivity of water.[27] Figure 4 shows that the thermal conductivity in the liquid phase is nearly identical to the thermal conductivity of water. The thermal conductivities of the sample in the supercooled state lie in the extrapolated region from the normal liquid phase. The thermal conductivities in the solid and liquid phases can be expressed as

$$\lambda_s = -1.973 \times 10^{-3}T + 1.079 \qquad (4)$$

for $-20 \le T \le 32$°C and

$$\lambda_l = 1.37 \times 10^{-3} T + 5.64 \times 10^{-1} \quad (5)$$

for $20 \le T \le 95$°C.

For distilled water and for $7 < T < 80$°C, our measured thermal conductivities were ±1.5% of the values given in Ref. 27. Because the measurement error for the thermal conductivity of water was ±1.5% (Ref. 28), the probable measurement error of the liquid thermal conductivity was ±3.0%. For quartz and for $-10 < T < 40$°C, our measured thermal conductivities were ±2.0% of the values given in Ref. 29. Reference 29 does not specify the measurement error for the thermal conductivity of clear quartz, and so we could not determine a probable measurement error for the solid thermal conductivity measured with the TPS technique.

Table 4 shows a comparison of the results of this work with the values listed in Refs. 10, 11, 30, and 31. The data in Ref. 30 are referenced in other sources, such as Refs. 11 and 31. Our measured thermal conductivities for the solid phase, $\lambda_s = 1.03$ W/m · K, are twice as large as the values given in Ref. 30. The measured λ_s are in the middle of the range of values given in Refs. 10 and 30, $\lambda_s = 1.6$ and 0.514 W/m · K. Our measured thermal conductivity for the liquid phases, $\lambda_l = 0.598$ W/m · K, are in the middle of the range of values given in Refs. 10 and 30, $\lambda_l = 1.0$ and 0.476 W/m · K. One possible reason for this difference of solid conductivities is the roughness of the solid samples used to measure thermal conductivity. Either a rough contact surface between the sample and the sensor or a porous sample will yield smaller apparent thermal conductivities than the actual thermal conductivity of the material. To prevent formation of either porous or rough surfaces, we solidified blocks of material near their melting point, very slowly onto a smooth glass plate. Therefore, we believe that the contact between the TPS sensor plates and our sample materials was sufficient to measure the true thermal conductivity of the material.

Table 5 shows a comparison of our estimated thermal conductivities with reference values, for various substances near their melting point. The data (Refs. 26 and 30–33) in Table 5 were estimated by extrapolation from the least-squares approximation of their original data. The top six materials shown in Table 5 indicate changes of up to a factor of 3, of their thermal conductivity near their melting points. On the other hand, the bottom four materials did not show a significant change of thermal conductivity near their melting points. The data from Ref. 33 were measured by using a hot-wire method for the liquid phase and by using a modified hot-wire method for the solid phase. The data of the Ref. 30 were measured by using a steady-state method with a disk sample. Table 6 shows a comparison of the thermal conductivities of water measured in this work with values from Refs. 28 and 30. Reference 28 contains internationally accepted values. As shown in Table 6, the measurement error of the data given in Ref. 30 was more than 21%. The data given in Ref. 26 were measured by using a hot-wire method. For the measurements done in both Refs. 30 and 26, the sample was solidified in a vessel around a temperature sensor. However, it seems to be difficult for a rigid sensor block or a fine wire sensor to stay in good contact with the sample because of the influence of thermal shrinkage of the sample. Therefore, the data in both Refs. 26 and 30 may contain significant measurement errors.

Table 4 Comparison of thermal conductivities of $Na_2HPO_4 \cdot 12H_2O$ measured in this work with values available in the open literature

		Thermal conductivity, W/m · K	
Reference	Temperature, °C	Solid	Liquid
This work	25	1.03	0.598
10	——	1.6	1.0
11	——	0.514	0.476
30, 31	32	0.514	——
	49	——	0.477

Table 5 Comparison of estimated thermal conductivities at the melting point from this work with values available in the open literature

			Thermal conductivity, W/m · K		
Substance	Reference	Melting point, °C	Solid (S)	Liquid (L)	Ratio (S)/(L)
$Na_2HPO_4 \cdot 12H_2O$	This work	35.54	1.01	0.613	1.64
H_2O	27, 32	0.00	2.09	0.565	3.70
$(C_6H_5)_2O$	33	27	0.264	0.125	2.10
$CH_3COO(CH_2)_{17}CH_3$	33	30	0.315	0.177	1.78
$C_6H_5C_6H_4OH$	33	58	0.306	0.154	1.98
$C_6H_5C_6H_5$	33	70	0.267	0.139	1.93
$Na_2HPO_4 \cdot 12H_2O$	30	36	0.497	0.510	0.98
$C_{10}H_7NH_2$	30	50	0.137	0.117	1.17
$CH_3C_6H_4NH_2$	30	44	0.125	0.126	1.00
$CH_3COONa \cdot 3H_2O$	26	58	0.514	0.446	1.15

Table 6 Comparison of thermal conductivity of water measured in this work with values available in the open literature

		Temperature, °C	
Description	Reference	25	45
Thermal conductivity, W/m · K	28 (±1.5%)	0.610	0.637
	This work	0.607	0.636
	30	0.569	0.506
Difference from Ref. 28, %	This work	−0.49	−0.16
	30	−6.7	−21.6

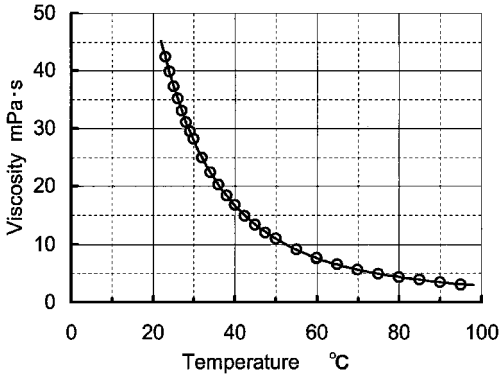

Fig. 5 Temperature dependence of viscosity of $Na_2HPO_4 \cdot 12H_2O$.

Viscosity

Figure 5 shows our measured viscosities. The solid curve in Fig. 5 represents a least-squares approximation to the data, which is

$$\eta = 1.15048 \times 10^{-12} T^6 - 4.87823 \times 10^{-10} T^5 + 8.60708 \times 10^{-8} T^4 - 8.16676 \times 10^{-6} T^3 + 4.47244 \times 10^{-4} T^2 - 1.38456 \times 10^{-2} T + 2.02476 \times 10^{-1} \quad (6)$$

for $23 \le T \le 95$°C.

Figure 5 indicates that the viscosity decreases monotonically with increasing temperature. The hydrate viscosity in the supercooled state lies in the extension of the curve from the liquid-phase region. With increasing degree of supercooling, the rate of increase of viscosity increases. Under supercooled conditions, the resulting high viscosity suppresses natural convection in the hydrate, causing heat loss from the hydrate to the surroundings to decrease. Therefore, for long-term energy storage applications, a supercooled hydrate is more effective than higher temperature hydrates.

To estimate the effect of the silicon oil on the viscosity measurement, we made the following comparison of the forces in the

Table 7 Comparison between the measured viscosity of water with and without silicon layer (measurement error: ±0.10 mPa · s)

	Viscosity of water, mPa · s			
		Measured		
Temperature, °C	Ref. 34 (±1%)	Without silicon (A)	With silicon (B)	(B) − (A)
1.0	1.733	1.815	1.815	0
5.0	1.522	1.595	1.573	−0.022
10.0	1.306	1.368	1.395	0.027
15.0	1.137	1.225	1.230	0.005
20.0	1.002	1.098	1.085	−0.013

Table 8 Relationship between sample temperature and measurement error of viscosity

Temperature range, °C	Rotational speed, rpm	Measurement error ± mPa · s
$23 \leq T < 30$	12	0.5
$30 \leq T < 38$	20	0.3
$38 \leq T < 50$	30	0.2
$50 \leq T < 55$	50	0.12
$55 \leq T \leq 95$	60	0.10

viscometer caused by the silicon oil and by the hydrate sample. Our measured coefficient of viscosity of the silicone was 48.6 mPa · s at 25°C, 26.3 mPa · s at 60°C, and 16.5 mPa · s at 95°C. The slip area between the hydrate and the spindle was 930 times wider than that between the silicon and the wire. The radius of gyration of the slip surface of the spindle in the hydrate was 25 times longer than that of the wire in the silicone. For the temperature range of our measurements, and assuming both the hydrate and the silicon to be Newtonian fluids, the torque for rotating the spindle in the sample ranged from 28,600 to 105,000 times larger than that for rotating the suspending wire in the silicon layer. Therefore, the influence of the silicon on the measurement of the viscosity was less than 0.003%.

Table 7 (see Ref. 34) shows a comparison of the viscosities of water measured with and without the silicon layer. For the measurements with water, the temperature was lower than for the measurements with the hydrate, so that the viscosity of the silicon was higher than for the measurement with the hydrate. In addition, the viscosity of water was lower than that of the hydrate. Although the resulting influence of the silicon layer on the measurement of the viscosity of water was, therefore, stronger than for the measurement of viscosity of the hydrate, no significant influence of the silicon on the measurement of the water viscosity was observed, indicating that there also was no significant influence for the measurement of the hydrate viscosity.

Because of the limited torque range of the motor driving the spindle, the accuracy of the viscosity measurement depends on the rotational speed of the spindle. The measurement accuracy depends on the temperature of the hydrate because, as shown in Fig. 5, the viscosity is temperature dependent. The relationship between the temperature of the hydrate, the maximum rotational speed, and the measurement error is listed in Table 8. For example, the measurement error of the viscosity is ±0.5 mPa · s over a range from 23 to 30°C.

Conclusions

To develop long-term latent energy-storage systems, Super-TES systems may use materials like disodium hydrogenphosphate dodecahydrate, which have a large heat of fusion, large degree of supercooling, and suitable melting point for applications such as space heating. Therefore, we measured the density, specific heat, thermal conductivity, and coefficient of viscosity of the hydrate within the temperature range most likely to be used for Super-TES systems. All of these properties of the hydrate are in the supercooled state, which can be extrapolated from the thermal properties in the non-supercooled liquid phase. The heat of fusion was smaller than most values reported in the open literature. The reason is that the original data are the heat of solidification calculated from smaller liquid specific heats than that measured by us. The density and the viscosity of the hydrate in the liquid phase decreased monotonically with increasing hydrate temperature. When the hydrate is used as a phase-change material, this indicates that it can be easily stratified in temperature.

The specific heat in the liquid phase and the thermal conductivity in the solid phase were twice as large as most values reported in the open literature. The reason may be that most specific heats reported in the open literature are overextrapolated values from the specific heat in the solid phase, and that the original data for the thermal conductivities reported in the open literature were measured with an instrument with large measurement error and without good contact of the sensor with the sample.

The large liquid specific heats that we measured indicate that the hydrate is useful for storing both latent and sensible heat. Under supercooled conditions, the viscosity increased significantly with decreasing temperature. This indicates that, under supercooled conditions, the increased viscosity decreases the strength of natural convection, which in turn decreases heat loss to the surroundings.

Acknowledgments

We thank Kyoto Electronics Manufacturing Company, Ltd., Kyoto, Japan and Hot Disk AB, Uppsala, Sweden for their helpful advice for measuring the thermal conductivity of liquids with the transient plane source method.

References

[1]Hirano, S., Saitoh, T. S., Oya, M., and Yamazaki, M., "Influence of Ultrasonic Vibration on Freezing Temperature of Hydrate," 34th Intersociety Energy Conversion Engineering Conf., Society of Automotive Engineers, Paper 1999-01-2617, Warrendale, PA, 1999.

[2]"Density of Water," *Chronological Scientific Tables 2000*, National Astronomical Observatory of Japan, Maruzen, Tokyo, 1999, p. 447.

[3]"12 Estimates of Uncertainties," *IAPWS Industrial Formulation 1997 for the Thermodynamic Properties of Water and Steam*, International Association for the Properties of Water and Steam, Palo Alto, CA, 1997, p. 46.

[4]Ditmars, D. A., Ishihara, S., Chang, S. S., and Bernstein, G., "Enthalpy and Heat-Capacity Standard Reference Material: Synthetic Sapphire (α-Al_2O_3) from 10 to 2250 K," *Journal of Research of National Bureau of Standards*, Vol. 87, No. 2, 1982, pp. 162, 163.

[5]"Specific Heat of Water at Constant Pressure," *Chronological Scientific Tables 2000*, National Astronomical Observatory of Japan, Maruzen, Tokyo, 1999, p. 564.

[6]Hirano, S., and Saitoh, T. S., "Long-Term Supercooled Thermal Energy Storage (Thermal Conductivity of $Na_2HPO_4 \cdot 12H_2O$," *Proceedings of the 37th National Heat Transfer Symposium of Japan*, Vol. 3, Heat Transfer Society of Japan, Tokyo, 2000, pp. 909, 910.

[7]Gustafsson, S. E., "Transient Plane Source Techniques for Thermal Conductivity and Thermal Diffusivity Measurement of Solid Materials," *Review of Scientific Instruments*, Vol. 62, No. 3, 1991, pp. 797–804.

[8]Gustavsson, M., Karawacki, E., and Gustafsson, S. E., "Thermal Conductivity, Thermal Diffusivity, and Specific Heat of Thin Samples from Transient Measurements with Hot Disk Sensors," *Review of Scientific Instruments*, Vol. 65, No. 12, 1994, pp. 3856–3859.

[9]Log, T., and Gustafsson, S. E., "Transient Plane Source (TPS) Technique for Measuring Thermal Transport Properties of Building Materials," *Fire and Materials*, Vol. 19, 1995, pp. 43–49.

[10]Kosaka, M., Asahina, T., and Taoda, H., "Phase Change Materials for the Thermal Energy Storage in Heating, Cooling, and Hot Water Supply System (Heat Storage VII)," Governmental Industrial Research Inst., Nagoya, Japan, Vol. 29, No. 2, 1980, p. 55.

[11]"Thermophysical Properties of Phase Change Materials for Heat Storage," *Handbook of Thermophysical Properties*, Japan Society of Thermophysical Properties, Yokendo, Tokyo, 1990, p. 119.

[12]Washburn, E. W. (ed.), "Latent Heats of Fusion," *International Critical Tables of Numerical Data, Physics, Chemistry and Technology*, Vol. 5, McGraw–Hill, New York, 1929, p. 131.

[13]Person, M. C. C., "Recherches sur la Chaleur Latente de Fusion," *Annales de Chimie et de Physique*, Vol. 27, 1849, pp. 250–272.

[14]"Melting Enthalpy of Substances," *Chronological Scientific Tables 2000*, National Astronomical Observatory of Japan, Maruzen, Tokyo, 1999, p. 567.

[15]Budavari, S. (ed.), "10175 Water," *The Merck Index*, 12th ed., Merck and Co., Whitehouse Station, NJ, 1996, p. 216.

[16]"Transition Enthalpy," *Handbook of Chemistry—Fundamental*, 4th ed., Chemical Society of Japan, Maruzen, Tokyo, 1993, p. II-244.

[17]"Properties of Fluids," *JSME Data Book: Thermophysical Properties of Fluids*, Japan Society of Mechanical Engineers, Tokyo, 1983, pp. 12, 13.

[18]Weast, R. C. (ed.), "Heat of Fusion of Some Inorganic Compounds," *CRC Handbook of Chemistry and Physics*, 55th ed., CRC Press, Cleveland, OH, 1974, p. B-244.

[19]"2.1 Melting Pressure of Ice I," *Pressure Along the Melting and the Sublimation Curves of Ordinary Water Substance*, International Association for the Properties of Water and Steam, Palo Alto, CA, 1993, p. 3.

[20]Roth, W. A., and Scheel, K. (eds.), "Spezifische Wärme c und Molekularwärme C anorganischer Stoffe," *Landolt-Börnstein Physikalisch-Chemische Tabellen*, 5th ed., Julius Springer, Berlin, 1923, p. 1259.

[21]Person, M., "Recherches sur la Chaleur Latente," *Comptes Rendus Hebdomadaires des Séances de L'Académie des Sciences, de L'Institut de France*, Vol. 23, 1846, pp. 162, 163.

[22]Washburn, E. W. (ed.), "The Heat Capacity of Chemical Compounds in The Crystalline State," *International Critical Tables of Numerical Data, Physics, Chemistry and Technology*, Vol. 5, McGraw–Hill, New York, 1929, p. 100.

[23]Nernst, V. W., "Untersuchungen über die spezifische Wärme bei tiefen Temperaturen II," *Sitzungsberichte der Königlich Preussischen Akademie der Wissenschaften*, Vol. 1910, 1910, pp. 262–282.

[24]Nernst, V. W., Koref, F., and Lindemann, F. A., "Untersuchungen über die spezifische Wärme bei tiefen Temperaturen I," *Sitzungsberichte der Königlich Preussischen Akademie der Wissenschaften*, Vol. 1910, 1910, pp. 247–261.

[25]Weast, R. C. (ed.), "Specific Heat of Water," *CRC Handbook of Chemistry and Physics*, 55th ed., CRC Press, Cleveland, OH, 1974, p. D-138.

[26]Inaba, H., Otake, H., Nozu, S., and Fukuda, T., "A Study on Latent Heat Storage Using a Supercooling Condition of Hydrate (1st Report, An Estimation of Physical Properties of Hydrate Sodium Acetate Including a Supercooling Condition)," *Transactions of the Japan Society of Mechanical Engineers*, Ser. B, Vol. 58, No. 553, 1992, pp. 204–212.

[27]"Thermophysical Properties of Ordinary Water," *JSME Data Book: Heat Transfer*, 4th ed., Japan Society of Mechanical Engineers, Tokyo, 1986, p. 331.

[28]"Appendix A. Critical Evaluated Experimental Data Reduced to the Saturation Line," *IAPS Formulation 1985 for the Thermal Conductivity of Ordinary Water Substance*, International Association for the Properties of Water and Steam, Palo Alto, CA, 1998, p. 7.

[29]"Thermophysical Properties of Fire-Proof Materials and Thermal-Insulation Materials," *VDI(Verein Deutscher Ingenieure)-WÄRMEATLAS*, Japan Management Association, Tokyo, 1988, p. De1.

[30]Lees, C. H., "On the Thermal Conductivities of Single and Mixed Solids and Liquids and Their Variation with Temperature," *Philosophical Transactions of the Royal Society of London, Series A: Physical and Mathematical*, Vol. 191, 1898, pp. 399–440.

[31]Washburn, E. W. (ed.), "Thermal Conductivity of Non-Metallic Liquids," *International Critical Tables of Numerical Data, Physics, Chemistry and Technology*, Vol. 5, McGraw–Hill, New York, 1929, p. 226.

[32]Washburn, E. W. (ed.), "Thermal Conductivity of Non-Metallic Solids," *International Critical Tables of Numerical Data, Physics, Chemistry and Technology*, Vol. 5, McGraw–Hill, New York, 1929, p. 216.

[33]Ohki, K., and Kowalczyk, L. S., "Thermal Conductivity of Some Organic Compounds at Their Melting Points," *Journal of Chemical and Engineering Data*, Vol. 9, No. 2, 1964, pp. 220, 221.

[34]"Appendix C: Viscosity Calculated for Water and Steam," *IAPS Formulation 1985 for the Viscosity of Ordinary Water Substance*, International Association for the Properties of Water and Steam, Palo Alto, CA, 1997, p. 15.